# The performance of inkjet-printed copper acetate based Hydrogen sulfide gas sensor on a flexible plastic substrate - varying ink composition and print density

Jawad Sarfraz [a,b], * Anna Fogde[a], Petri Ihalainen[a], Jouko Peltonen[a]

[a]Laboratory of Physical Chemistry, Center for Functional Materials, Åbo Akademi University, Porthaninkatu 3-5,FI-20500 Turku, Finland.

[b]Nofima - Norwegian Institute of Food, Fisheries and Aquaculture Research, P.O. Box 210, NO-1431 Ås, Norway

*E-mail: jsarfraz@abo.fi

## 1 Abstract

Low-cost and robust hydrogen sulfide ($H_2S$) gas sensors can be utilized in different industrial applications. Earlier we have demonstrated an inexpensive wirelessly readable copper acetate based $H_2S$ gas sensor which was successfully employed for monitoring the quality of raw poultry. In this study we have thoroughly investigated and optimized the performance of inkjet-printed copper acetate based $H_2S$ gas sensor on flexible plastic substrate at room temperature. The effect of ink composition, print density, number of print nozzles and temperature of the substrate on sensor performance was tested. The long term stability of these sensors after exposure to $H_2S$ was studied extensively and was optimized as a function of the print density of copper acetate. The conversion of copper acetate to copper sulfide upon reaction with $H_2S$ was established by x-ray photoelectron spectroscopy. We believe that the optimized sensor developed in this study with respect to stability, repeatability and material consumption will pave the way for the commercial use of these sensors e.g. in food quality monitoring and environmental applications.

## 2 Introduction

Low-cost gas sensors and indicators have attracted a lot of attention in the recent years. Gas-sensitive films have been developed for potential use in e.g. healthcare and diagnosis, food quality control, defense, anti-terrorism and environmental controls et cetera. Among different gases, hydrogen sulfide ($H_2S$) is responsible for many incidents of occupational toxic exposure. [1] $H_2S$ is a toxic and flammable gas and the clinical effects of $H_2S$ depend on its concentration and the duration of exposure. [1] Although $H_2S$ has a distinctive rotten egg smell, above concentrations of 100 ppm it is practically undetectable by smell due to saturation of olfactory nerves. $H_2S$

above concentrations of 100 ppm poses serious health risks, including shock, irritation of the eyes, skin and respiratory paralysis. Concentrations above 500 ppm are immediately fatal as it affects the uptake of oxygen in the blood.

A commercial optical indicator for the detection of $H_2S$ is based on lead acetate paper strips. These strips turn from white to grey when exposed to $H_2S$. More recently bismuth based optical indicators were developed to detect very low concentrations of $H_2S$ in small sample volume.[2] These indicators are mainly used for qualitative detection of $H_2S$ in water, air or breath. Commonly, sensors consisting of metal oxides, doped metal oxides[3],[4],[5] and conducting polymers[6], [7] have been employed for the detection of $H_2S$. These sensors typically change their resistance upon exposure to $H_2S$. However, the fabrication of these sensors involves complicated synthesis steps which are normally not up scalable. Furthermore these sensors are generally sensitive to temperature and humidity.[8] Thus these devices are expensive to fabricate on large scale and cannot be used in e.g. food packaging

Intelligent food packages equipped with sensors which can monitor the quality of food in real time is a very interesting concept. Upon bacterial degradation of poultry meat often sulfur containing bacterial metabolites is produced including $H_2S$. [9],[10],[11] Poultry meat is usually packed in modified atmosphere and the humidity level inside the package is quite high. For practical use, a sensor which can monitor the quality of poultry meat by reacting with volatile bacterial metabolites should be compatible with high humidity conditions, modified atmosphere (either $CO_2$ modified or vacuum) and low temperatures (refrigerator temperature around +6 $^{\circ}$C) of the package. Furthermore the sensor response should be irreversible memory based, it should be mass producible, and have low manufacturing and operating cost. Simple copper acetate based irreversible memory based chemiresistive type sensor full fills all these requirements.

It is well reported in literature that copper acetate reacts with hydrogen sulfide both in solution and solid state, in water it reacts to produce a black precipitate of copper sulfide while in organic solutions it produces organosols. [12], [13], [14] Copper acetate based films have shown to be very promising for the irreversible chemiresistive detection of $H_2S$ gas. Over eight orders of magnitude change in resistance was reported when these films were exposed to as low as 1 ppm $H_2S$. Furthermore the sensitivity of copper acetate films towards $H_2S$ was further improved to sub ppm levels by using copper acetate gold nanoparticle composite film and subsequent plasma treatment.[15] This substantial and irreversible change in resistance at room temperature was explained by the difference in conductivity between copper acetate which is insulating and the reaction product copper sulfide which is conducting. [16], [17] Moreover the conductivity of copper sulfide depends upon the stoichiometric ratio of copper and sulfur.

We have studied the performance parameters of printed copper acetate based $H_2S$ sensors in detail. The onset time of detection, selectivity, sensitivity, effect of humidity and long term stability for these sensors were studied and has been reported earlier. [16] A demonstration of copper acetate based $H_2S$ sensor for monitoring the quality of raw poultry has been reported,

where we have integrated the sensor with a printed planar coil antenna and a printed capacitor to construct an inexpensive, wirelessly readable printed RLC (R = resistance, L = inductance, C = capacitance) circuit. [18] This circuit was designed with an operational frequency of 8.2MHz.This frequency is desirable because of the availability of commercial readers. The threshold resistance with respect to the quality factor of the circuit was 10KΩ. In this case no power source is required and the status of the sensor can be confirmed easily by a hand held EAS reader.[18] The sensing films were also fabricated by printing which enables large scale manufacturing and precise control of film quality (e.g. film coverage, roughness and thickness). Furthermore, it has been shown that by the selection of the substrate like polyethylene terephthalate (PET), a nonporous plastic, the humidity background of these sensors can be minimized. [18] For this circuit to work properly the stability of the sensor are very important, meaning the sensor should retain its resistance level after exposure to $H_2S$ to avoid false positive.

In this study we have thoroughly investigated and optimized the performance of inkjet-printed copper acetate based $H_2S$ gas sensor on flexible plastic substrate by varying ink composition and print density. The wettability of the substrate by sensing ink regarding varying ink composition is studied by following the contact angles and is explained in terms of surface energy of the substrate and surface tension of the sensing inks. The effect of parameters like multiple nozzles vs single nozzle printing and printing with and without a heating plate on sensor performance was also tested. The long term stability of these sensors after exposure to $H_2S$ was studied extensively and optimized as a function of the print density of copper acetate. The conversion of copper acetate to copper sulfide upon reaction with $H_2S$ was established by x-ray photoelectron spectroscopy.

# 3 Materials and methods

## 3.1 Fabrication of the sensing film on a PET substrate

The fabrication process of the sensor on a PET substrate has been explained earlier; [18] briefly the interdigitated electrodes on PET were fabricated completely in a commercial roll-to-roll manufacturing process. The electrodes were made by etching the wire structures on the copper-coated PET film. The thickness of the PET film and copper layer were 50 μm and 18 μm, respectively. The copper fingers in the active area of the sensors and contacting pads were protected against oxidation by coating them with gold. Consecutive layers of nickel and gold were applied by electroplating on the copper surface. The purpose of the nickel layer was to provide good adhesion for gold. To minimize the amount of gold, a patterned 15 μm thick PDMS-film was screen-printed on the copper structures and the parts of the copper fingers free of PDMS were coated with gold.

The copper acetate based sensing inks were prepared by dissolving the copper acetate salt in a mixture of water, ethylene glycol (EG) and 2-propanol (IPA) or in a mixture of water and 2-butoxyethanol (BE). Copper acetate, EG and IPA were bought from Sigma Aldrich and 2-

butoxyethanol was from Acros. All the chemicals were used as received. Inkjet printing was performed using a Dimatix Materials Printer (DMP-2831). The printing was done in ambient conditions using either a single nozzle or four nozzles simultaneously, with drop volume 10 pL, firing voltage 27 ± 3 V and a custom waveform to ensure optimal droplet formation. Surface tension of the solvents was measured with a Sensadyne PC 9000 Bubble tensiometer, viscosity was measured with an Ostwald viscometer and the density was measured with an Anton-Paar DSA 5000 Densitometer.

### 3.2 $H_2S$ sensing experiments

A gas cylinder with 200 ppm $H_2S$ gas mixture in nitrogen was used as a $H_2S$ source. A resistance measurement chamber consisted of an aluminum box with the dimensions 20 cm × 20 cm × 12 cm. The box was equipped with four wolfram probes, an electrochemical $H_2S$ sensor (AlphaSense, with operation range of 0–200 ppm and response time <35 s), a humidity and a temperature sensor (Sensirion SHT75, with a response time of 8 s). The resistance of the sensor was followed by a two-point method by connecting the probes with a digital multimeter (Keithley 2100).

### 3.3 X-ray photoelectron spectroscopy

X-ray photoelectron spectroscopy (XPS) spectra were obtained with a PHI Quantum 2000 scanning spectrometer, using monochromatic Al Kα x-ray source (1486.6 eV) excitation and charge neutralization by using electron filament and an electron gun. The photoelectrons were collected at 45° in relation to the sample surface with a hemispherical analyzer. The analyzing depth was approximately 5 - 10 nm. The pass energy was 187.85 and 58.7 eV for survey and high resolution spectra, respectively. The measurements were carried out on three different spots for each sample. The atomic concentration (at.%) of the different elements was derived by calculating the area of the peaks and correcting for the sensitivity factors using the software MultiPak v6.1A from Physical Electronics.

### 3.4 Contact angle and surface energy determination

A CAM 200 contact angle goniometer (KSV Instruments Ltd., Finland) was used for the determination of contact angles of liquids and formulations on the sample surface. The measurements were done at ambient conditions (T = 22 ± 2°C, RH = 25 ± 2%). The surface energy of the substrate was calculated by the Owens, Wendt, Rabel and Kaelble (OWRK) method, by measuring the contact angles of water, ethylene glycol and diiodomethane on the substrate.

## 4 Results and discussion

### 4.1 Ink formulation for inkjet printing

Three different ink formulations were made using mixed solvents. Water, ethylene glycol and isopropanol were used in the volume ratios 7:2:1 (formulation A) and 6.5:1.5:2 (formulation B)

respectively and water and 2-butoxyethanol were used in the volume ratio 4:1 (formulation C). The properties of the formulations were measured as a function of temperature and the results are collected in

Table **1**.

Table 1: Ink formulation properties as a function of temperature and Z number

| **T (°C)** | | | | | |
|---|---|---|---|---|---|
| **Formulation A** | **η (Pa s)** | **ρ (Kg/m$^3$)** | **Nozzle diameter, d (m)** | **γ (N/m)** | **Z** |
| **20** | 0.00262 | 1014.9 | 21.5x10$^{-6}$ | 0.039 | 11.1 |
| **25** | 0.00224 | 1012.5 | 21.5x10$^{-6}$ | 0.038 | 12.9 |
| **30** | 0.00194 | 1010.0 | 21.5x10$^{-6}$ | 0.038 | 14.8 |
| **35** | 0.00169 | 1007.4 | 21.5x10$^{-6}$ | 0.038 | 16.9 |
| **40** | 0.00147 | 1004.7 | 21.5x10$^{-6}$ | 0.037 | 19.3 |
| **Formulation B** | | | | | |
| **20** | 0.00323 | 995.5 | 21.5x10$^{-6}$ | 0.031 | 7.9 |
| **25** | 0.00270 | 992.6 | 21.5x10$^{-6}$ | 0.030 | 9.4 |
| **30** | 0.00228 | 989.6 | 21.5x10$^{-6}$ | 0.029 | 11.0 |
| **35** | 0.00185 | 986.5 | 21.5x10$^{-6}$ | 0.029 | 13.5 |
| **40** | 0.00160 | 983.4 | 21.5x10$^{-6}$ | 0.029 | 15.5 |
| **Formulation C** | | | | | |
| **20** | 0.00198 | 990.2 | 21.5x10$^{-6}$ | 0.030 | 12.7 |
| **25** | 0.00172 | 987.7 | 21.5x10$^{-6}$ | 0.029 | 14.3 |
| **30** | 0.00153 | 985.2 | 21.5x10$^{-6}$ | 0.028 | 15.9 |
| **35** | 0.00141 | 982.5 | 21.5x10$^{-6}$ | 0.027 | 17 |
| **40** | 0.00135 | 979.7 | 21.5x10$^{-6}$ | 0.026 | 17.6 |

Parameter Z is a dimensionless number which is the inverse of the Ohnesorge number (Oh) and can be used to estimate the printability of the inks.

$$Z = (\gamma \rho d)^{½} / \eta$$

where ρ, η and γ are the density, dynamic viscosity and surface tension of the fluid and d is the nozzle diameter. Z number is often related to the printability of the inks. According to Fromm [19] and Reis [20] a range of $1 < Z < 10$ represents good printability. However, Jang et al have used different mixtures of ethanol, water and ethylene glycol and according to them a Z number range $4 < Z < 14$ was suitable for printability. [21] According to Z-values in Table 1, the ink formulations A, B and C were suitable for inkjet printing at room temperature as shown in Figure 1.

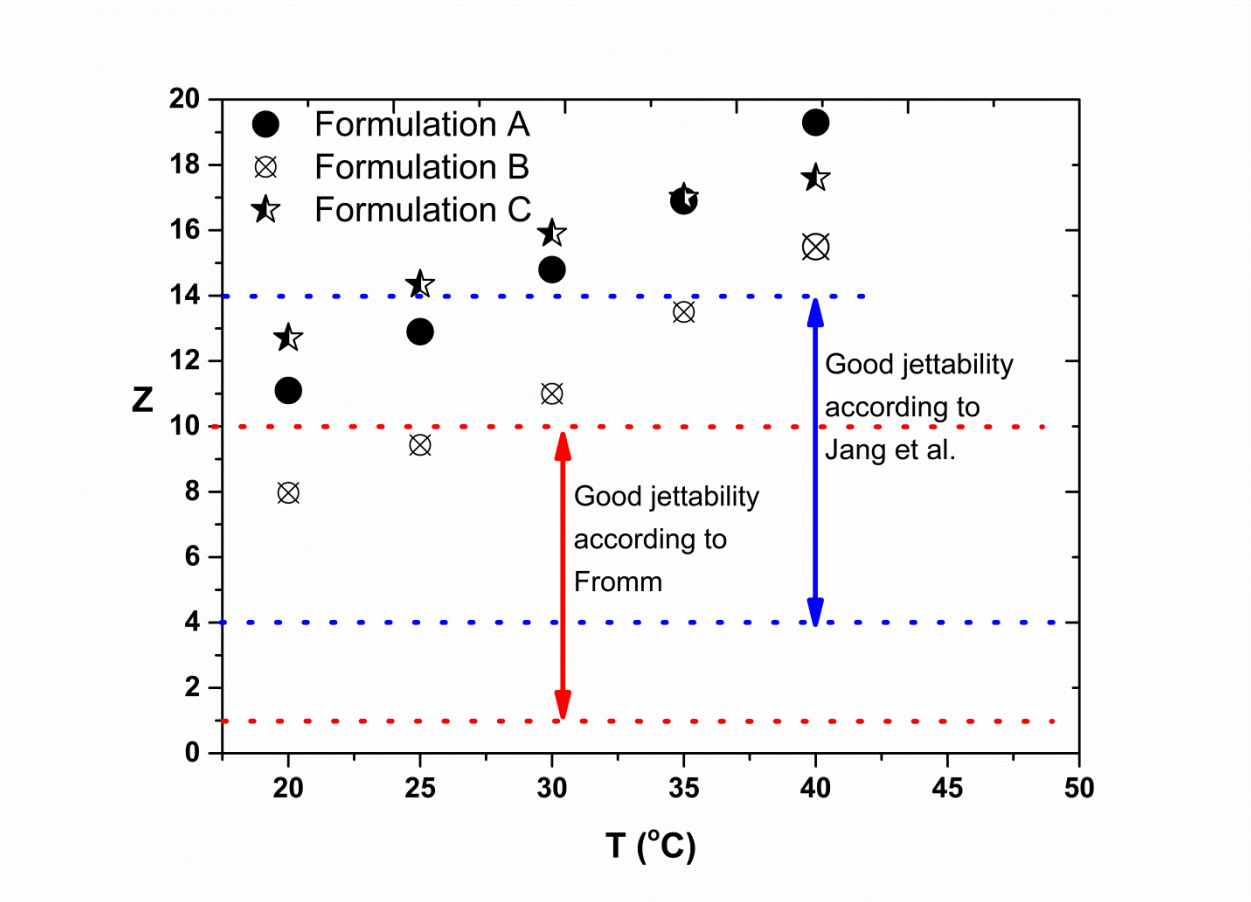


Figure 1: The Z number as a function of temperature for ink formulations A, B and C.

## 4.2 Fabrication of sensing film and performance

$H_2S$ sensing film "type A" was prepared by inkjet printing of 0.1M copper acetate solution of formulation A. The print density of the film was 3362 drops / $mm^2$. Seventeen of these sensing films were then exposed to 10 ppm $H_2S$ gas (at RH 40±5 %) for one hour. The initial resistance of these sensing films was more than 1 GΩ. The saturation resistance after the exposure to $H_2S$ was noted. The average resistance of the sensing films after exposure to $H_2S$ was 1308 Ω with standard deviation of 1350 Ω which shows that there is a large variation in the saturation resistances among individual sensors. (Supporting material Table 1) The reproducibility of these uniformly prepared sensors (type A) when exposed to $H_2S$ under similar conditions was hence rather poor.

Similarly, sensing film type B was prepared by inkjet printing of 0.1M copper acetate solution of formulation B. Sensors were made by first air plasma treating the substrate (for 2 minutes) and then by printing films with print density of 2601 drops / $mm^2$. The air plasma treatment was performed to clean the surface from organic impurities before printing. Fifteen of these sensors were then exposed to 10 ppm $H_2S$ gas (at RH 40±5 %) for one hour. The initial resistance of also these sensors was more than 1 GΩ. The average resistance of the sensors after exposure to $H_2S$ was 20Ω with standard deviation of 7.5Ω. (Supporting material Table 2) The very small standard deviation (considering $\Delta R > 10^8$ Ω) shows that these sensors have very good reproducibility even with less print density compared to sensors A.

Several sensing films (type B) with varying print densities were then prepared by printing different amounts of 0.1M copper acetate solution in formulation B (i.e. 441, 529, 676, 900, 1156, 1323, 1681 and 2601 drops / $mm^2$). In this case the substrate was not subjected to plasma treatment before printing. These sensing films were exposed to 10 ppm $H_2S$ gas (at RH 40±5 %) for one hour. For these sensors to be used in intelligent food packaging the saturation resistance after $H_2S$ exposure should drop less than 10KΩ threshold resistance and the sensor should also retain its resistance value as explained earlier. Once exposed to $H_2S$ the resistance of these sensors can increase in air due to surface oxidation which is undesirable. The reproducibility (in terms of average saturation resistance and standard deviation) and long-term stability (By storing these $H_2S$ exposed sensing films in air for 30 days) of these sensors were tested and the results are summarized in Table 2.

Table 2: Reproducibility and long term stability of sensor B as a function of print density when exposed to $H_2S$

| Print density (drops/$mm^2$) | Average saturation resistance (Ω) | Standard deviation (SD) | Relative change after 30 days (in ambient) |
|---|---|---|---|
| **441** | **610200** | **613013** | **OVLD*** |
| **529** | **88680** | **113863** | **OVLD*** |
| **676** | **561** | **284** | **+25%** |
| **900** | **476** | **237** | **+10%** |
| **1156** | **97** | **66** | **+10%** |
| **1323** | **152** | **52** | **+10%** |
| **1681** | **25** | **3** | **±0%** |
| **2601** | **20** | **7** | **±0%** |

*OVLD = R >$10^8$ Ω

It can be seen in Table 2 that the sensor stability and reproducibility is affected by the print density. The sensors with high print densities (relatively thicker films) have very small standard deviation and they remain stable after exposure to 10 ppm $H_2S$. On the contrary, the sensors with low print densities (thinner films) have relatively high standard deviation and their resistance has changed significantly during the 30 days of storage period after exposure to 10 ppm $H_2S$ in ambient conditions. The change in resistance of the copper acetate based sensing films upon exposure to $H_2S$ is related to the formation of copper sulfide. Copper sulfide is a stable compound at room temperature. However, during the chemical reaction between copper acetate and $H_2S$ intermediate products can also be produced, e.g. $Cu_2S$, $Cu_{1.96}S$, $Cu_xS$ ($1<x<2$), CuS & $CuS_2$. [17] The stability and the conductivity of the copper sulfide film depend on the stoichiometric ratio between sulfur and copper and on the crystallinity of copper sulfide. [22] One other possible

explanation for the instability and high saturation resistance of relatively thinner films can be the poor film quality (less coverage) and oxidation of copper sulfide film with time.

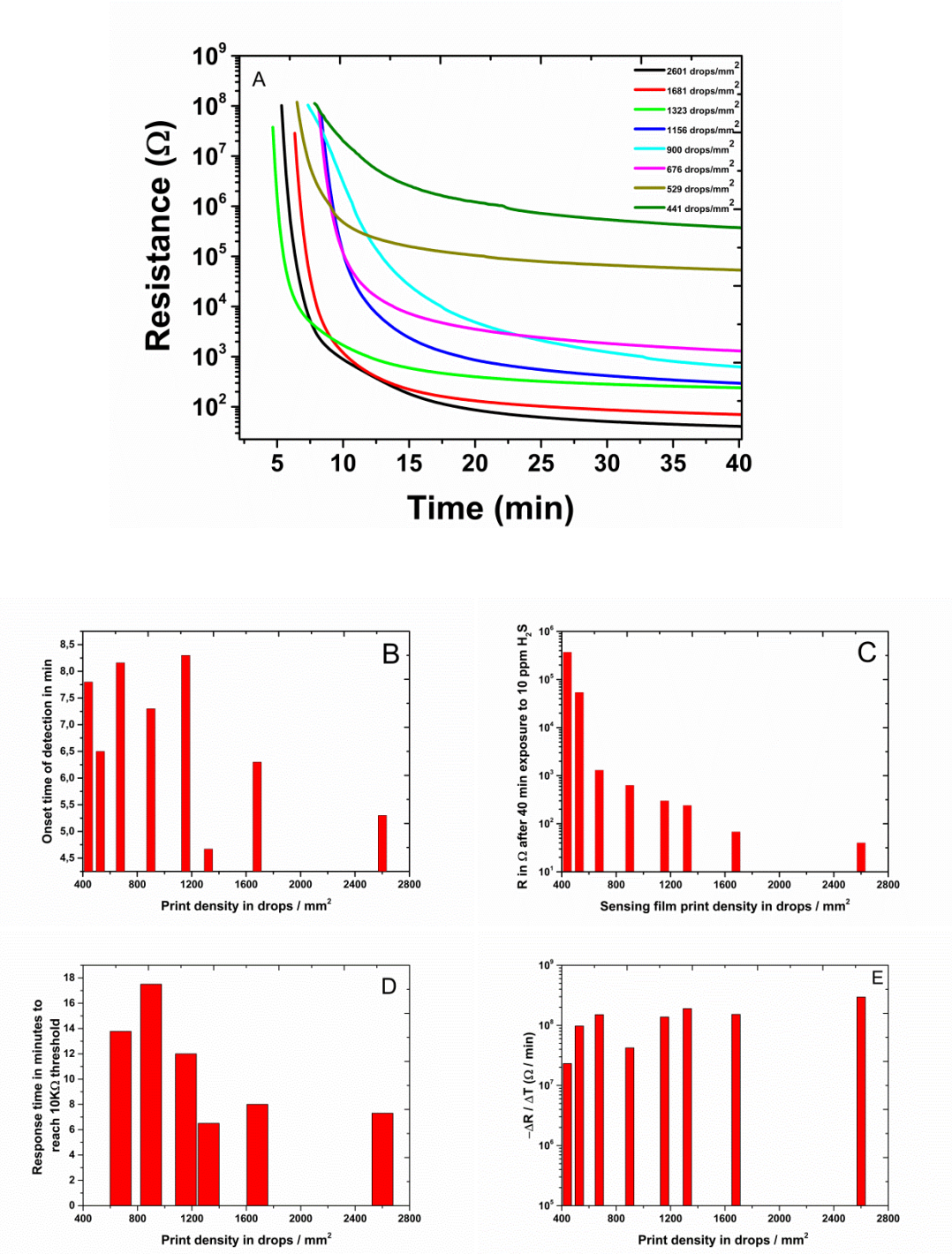


Figure 2: (A) Change in resistance of copper acetate films with different drop densities (sensor B) as a function of time when exposed to 10 ppm $H_2S$ at RH 40±5 % (B) onset time of detection as a function of print densities towards 10 ppm $H_2S$ (C) saturation resistance after 40 minutes of exposure towards 10 ppm $H_2S$ as a function of print density (D) response time to reach 10KΩ

threshold as a function of print density and (E) rate of change of resistance to reach 5MΩ level as a function of print density.

The response towards 10 ppm $H_2S$ (at RH 40±5 %) of sensors of type B with different print densities is presented in Figure 2A. It can be seen that the sensors with print densities 441 drops / $mm^2$ and 2601 drops / $mm^2$ have the highest and lowest saturation resistances of 360 KΩ and 40 Ω, respectively, after 40 minutes exposure to $H_2S$ (Figure 2A and Figure 2C). A clear trend of decreasing saturation resistance as a function of increasing print density is observed in Figure 2C. This can be explained by the improved coverage and the formation of a uniform film between the interdigitated electrodes with increasing film density. Moreover, very low saturation resistance in case of sensing film with print density 2601 drops / $mm^2$ can be explained with the formation of a more conducting phase of copper sulfide (CuS & $CuS_2$).

The onset time of detection which is defined as, "the time that it takes for the sensor to respond to the presence of the analyte" [23] lies in the range of 4 to 8 minutes (Figure 2B) for all the sensors. The sensor with intermediate print density of 1323 drops / $mm^2$ showed the onset time of detection of 4.6 minutes which is almost twice as fast compared to the sensing film with intermediate print density of 1156 drops / $mm^2$ (8.3 minutes). These variations in the onset time of detection between the two films which are very close to each other in terms of print densities can be associated with the printing variations (due to bulging etc.) and resulting effects on the connectivity of the copper sulfide particles between the interdigitated electrodes.
The response time of sensors (type B) to reach 10KΩ threshold as a function of print density is shown in Figure 2D. The sensing films with low print density of 441 and 529 drops/$mm^2$ did not reach the level of 10KΩ. The sensing films with relatively high print density of 1323, 1681 and 2601 drops/$mm^2$ have response time of 6.5, 8 and 7.3 minutes respectively to reach a resistance level of 10KΩ. A trend of improved response time as a function of print density of the sensing film can be seen in Figure 2D. Figure 2E shows the rate of change of resistance of the sensing films to reach 5MΩ level as a function of print density. There is almost one order of magnitude difference in the rate between the film with lowest and highest print density, the former being one order of magnitude faster than the later. Overall the sensing films (type B) with print density of 1323, 1681 and 2601 drops/$mm^2$ are optimum with respect to reproducibility (in terms of standard deviation and average values), stability in air, onset time of detection, response time, rate of change in resistance and saturation resistance.

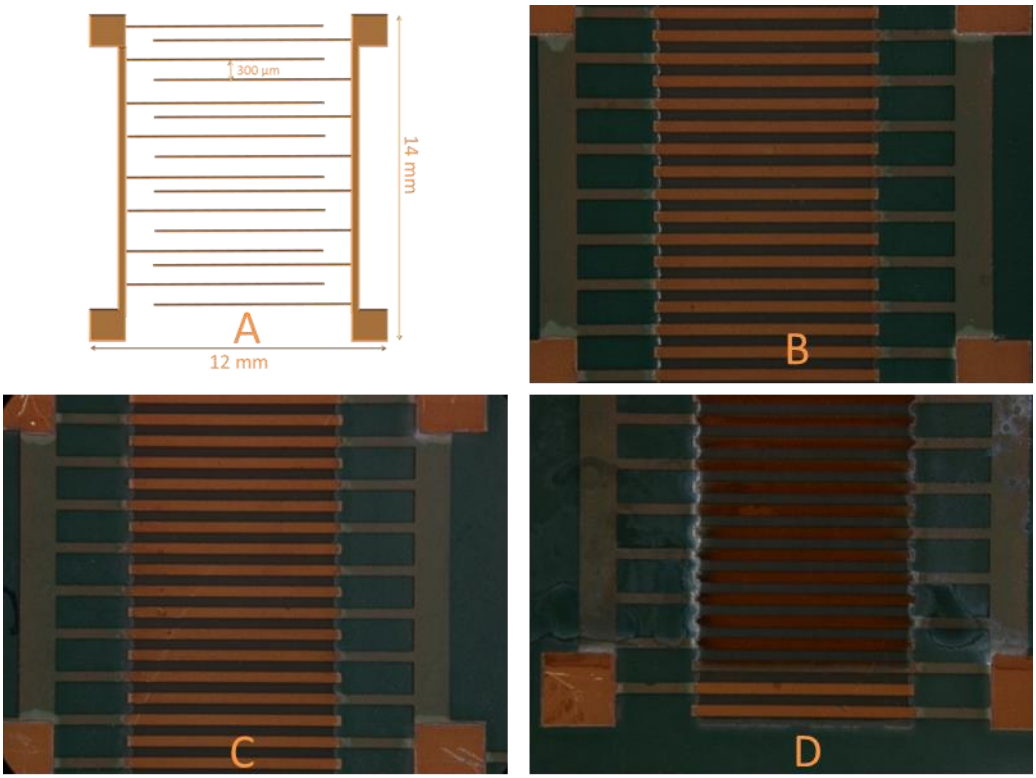


Figure 3: (A) A scheme showing the interdigitated electrodes with total dimensions 12mm x 14mm, distance between the electrodes and the width of the fingers being 300 µm, (B) A picture of the interdigitated electrodes on a PET substrate, (C) A picture of the $H_2S$ exposed sensor B with print density 441 drops / $mm^2$ and (D) A picture of the $H_2S$ exposed sensor B with print density 2601 drops / $mm^2$

Figure 3A and Figure 3B show the scheme and a picture of the interdigitated electrodes on a PET substrate and Figure 3C and Figure 3D show $H_2S$ exposed copper acetate film with print densities 441 and 2601 drops / $mm^2$, respectively. The dimensions of the electrode structure was 12mm x 14 mm and the distance between the electrodes was 300 µm (Figure 3A). In Figure 3D a clear color contrast can be seen at the interdigitated electrodes. The electrodes with the printed sensing film appear darker than the unprinted interdigitated electrodes. Furthermore shining spots can be seen in Figure 3D which can be related to the formation of a more conducting phase of copper sulfide. On the other hand, probably a very thin film may have been formed with the print density of 441 drops / $mm^2$ (Figure 3C) which may explain why it appears very similar to the unprinted interdigitated electrodes. Moreover, no shining spots can be seen in Figure 3C which explains the high saturation resistance of these films after exposure to $H_2S$ and their poor long term stability.

Apart from ink formulations A and B, a third formulation C consisting of water and BE with a volume ratio 4:1 was developed with optimized surface tension and viscosity for inkjet printing. A number of sensors were then prepared by printing different amounts of 0.1M copper acetate solution of formulation C (i.e. 1156, 1681, 2601 and 4624 drops / $mm^2$) to produce sensing films with different print densities. These sensors were then exposed to 10 ppm $H_2S$ gas (at RH 40±5 %) for two hours. The responses of these sensors are shown in Figure 4. It can be clearly seen

that the performance of the sensors of type C was poor compared to that of sensor type B in terms of both sensing kinetics and saturation resistance. These sensing films (type C) were unstable in air irrespective of the print density. After exposure to $H_2S$, when these sensing films (type C) are stored in air under ambient conditions, the resistance of all the films was increased to more than 100 MΩ within 48 hours. Furthermore, none of the sensing films (type C) was able to reach the 10KΩ threshold. The poor sensing response of sensor type C of may be explained by the fact that BE has properties similar to surfactants and has a high boiling point of 171°C. It may be that after inkjet printing of the sensor, the presence of BE caused hindrance in the reaction between copper acetate and $H_2S$ gas and furthermore interrupted the formation and growth of copper sulfide crystals.

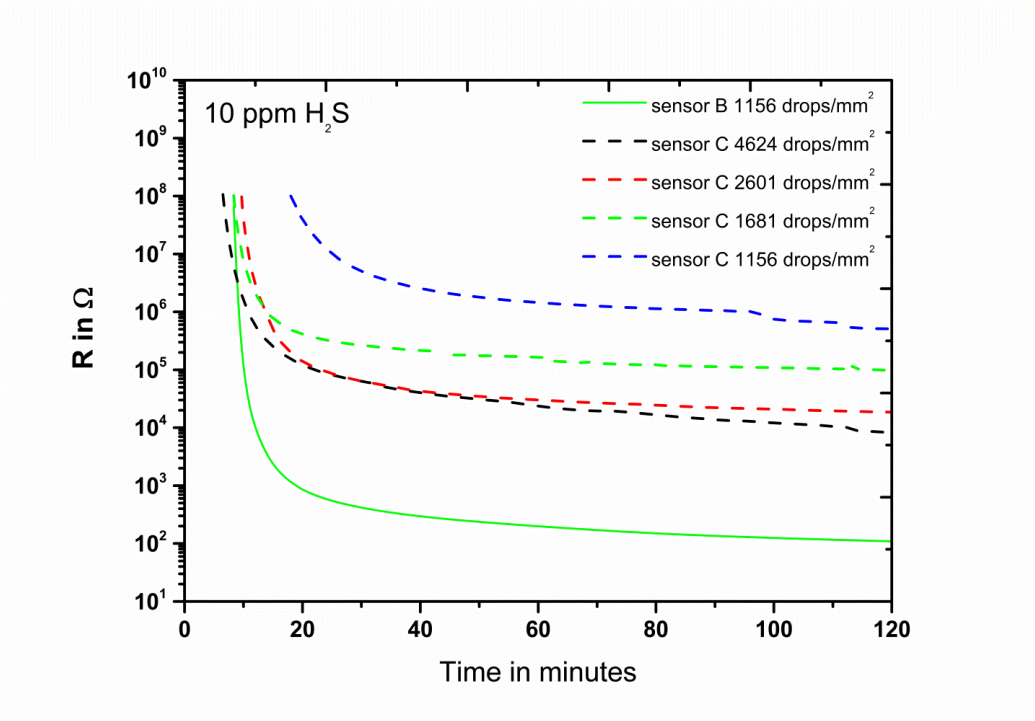


Figure 4**:** Change in resistance of copper acetate films with different drop densities (sensor C) as a function of time when exposed to 10 ppm $H_2S$ at RH 40±5 %.

The response of sensors type A, B and C towards $H_2S$ can be further explained in terms of the surface energy of the substrate, the ink surface tension and their polar / non-polar nature. The PET substrate is non-polar in nature. The surface energy of the substrate was found to be 49.3 $mJ/m^2$ with the values of the polar and dispersive component of 1.5 $mJ/m^2$ and 47.8 $mJ/m^2$, respectively. The contact angle values are listed in Table 3.

Table 3: Contact angle values of different liquids on the PET substrate.

| | **Contact angle on PET substrate** |
|---|---|
| **Water [°]** | 73±1 |
| **Ethylene glycol [°]** | 61±1 |

| | |
|---|---|
| **Diiodomethane [°]** | 20±1 |
| **2-Butoxyethanol [°]** | 11±0.5 |
| **Isopropyl alcohol [°]** | 0 |
| **Formulation A [°]** | 64±2 |
| **Formulation B [°]** | 18±1 |
| **Formulation C [°]** | 11±0.5 |

The ink formulations A and B have same components (water, EG and IPA) but in different ratios, resulting in significant differences in the surface tensions of the formulations (Table 1) as well as contact angles of these formulations with the substrate (Table **3**). Formulation A has a higher surface tension (0.039 N/m) and contact angle (64°) value. The lower amount of IPA in formulation A explains the higher contact angle (partial wetting) with the substrate. It is well known in literature that an unstable printing is obtained within the suitable drop spacing range where the contact angle of the ink at the substrate is greater than the advancing contact angle due to the formation of irregular bulge. [24], [25], [26] Due to this bulging effect a poor and macroscopically heterogeneous film was obtained by ink formulation A, which further explains the poor response of sensor type A towards $H_2S$ (in terms of stability and repeatability).

Formulation B, however, has twice the amount of IPA compared to formulation A which explains its lower surface tension (0.031 N/m) and contact angle value (18°). The better wetting of the substrate in the case of formulation B improved the quality of the printed film with reduced bulging. After exposure of the sensor type B towards $H_2S$, the formation of conducting copper sulfide crystals and percolation in the continuous conducting networks explains the significantly better sensing response of sensor type B towards $H_2S$.

The composition of formulation C was different than that of A and B, here BE was mixed with water instead of EG and IPA. Formulation C has the lowest surface tension (0.030 N/m) and contact angle (11°) values. Ink formulation C resulted in more uniform and thin films compared to ink formulation B due to better wetting of the substrate. However, sensor C showed poor response towards $H_2S$ compared to sensor B (Figure **4**). Even though sensor C showed improved sensing response towards $H_2S$ as a function of print density (Figure **4**), the fact that all the sensors C (irrespective of print density) were unstable after exposure to $H_2S$ might be explained by the formation of unstable amorphous semiconducting phases of copper sulfide and oxidation of the thin film after exposure to $H_2S$. [22]

The effect of parameters like multiple nozzles vs single nozzle printing and printing with and without heating plate on sensor performance was also tested. Both the sensors type B prepared by either single nozzle or with four nozzles simultaneously (print density 900 drops / $mm^2$) were identical when exposed to 10 ppm $H_2S$ in terms of saturation resistance, sensing kinetics and onset time of detection (results not shown). However, there was a slight difference in the saturation resistance between the two sensors B prepared with and without a heating plate (single

nozzle printing) as shown in Figure 5. The sensor prepared without substrate heating has slightly lower saturation resistance compared to the sensor prepared with substrate heating at 60$^{O}$C. In terms of sensing kinetics and onset time of detection both sensors were quite similar. The difference in the saturation resistance can be explained by the fact that the ink formulation contained ethylene glycol. Ethylene glycol has a boiling point around 200 $^{O}$C and at room temperature the evaporation is fairly slow. It is possible that the sensor prepared at room temperature might contain ethylene glycol even after 24 hours of drying. This not only facilitated the adsorption of $H_2S$ at the surface of the sensor but also assisted the formation and growth of copper sulfide crystals. This in turn led to better conductivity compared to the sensor prepared with substrate heating at 60$^{O}$C.

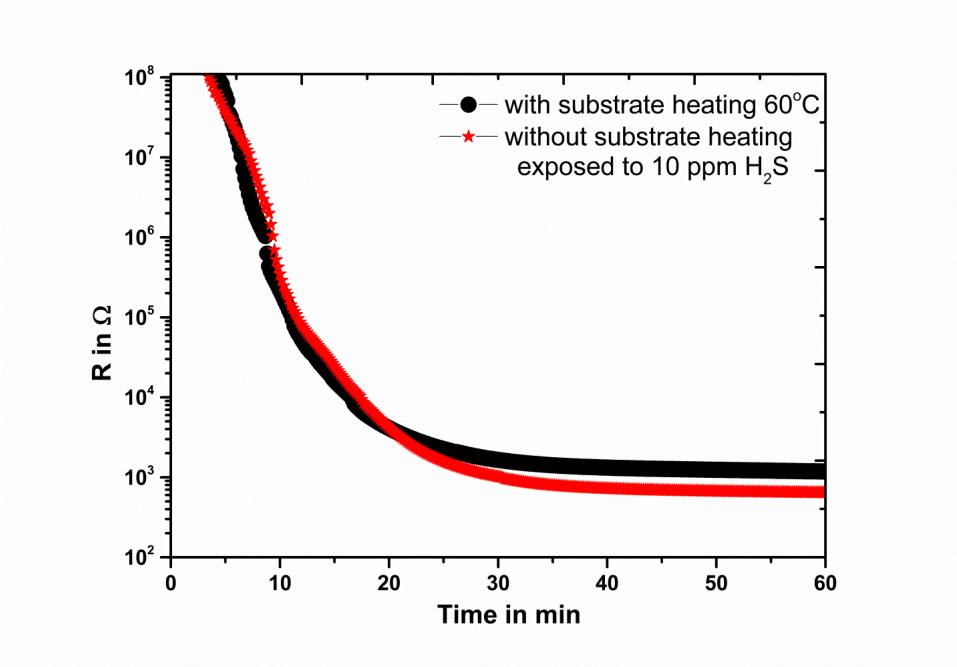


Figure 5: Change in resistance of sensor B as a function of time when exposed to 10 ppm $H_2S$. The sensors were prepared with and without heating at 60$^{o}$C.

## 4.3 XPS

The formation of copper sulfide upon reaction of the copper acetate film with $H_2S$ was confirmed with x-ray photoelectron spectroscopy. Figure **6**A shows the survey spectrum of sensor B (print density 2601drops / mm$^2$) being exposed to $H_2S$ (10 ppm for one hour). In Figure **6**A clear peaks of copper, sulfur, carbon and oxygen can be seen. Furthermore, the atomic ratio of 2.15 between sulfur and copper shows that copper sulfide is sulfur abundant which explains the high conductivity of the film after reaction with $H_2S$.

The binding energies are determined relative to C1s peak (284.6 eV) as shown in Figure **6**B. The high-resolution peak of Cu $2P^{3/2}$ is shown in Figure **6**C. The peak position of 932.5 eV shows that copper is bound with sulfur in the form of copper sulfide.[27] Furthermore it can be seen in Figure **6**C that no “shake up” satellite is visible which shows that copper is most likely present in its

reduced state (+1 oxidation state instead of +2).[28] The high resolution spectra of sulfur (S2p, Figure **6**D) further confirm the formation of copper sulfide. [29] The peak position of 169.5 eV shows a small amount of surface oxidation and conversion of copper sulfide into copper sulfate.[30]

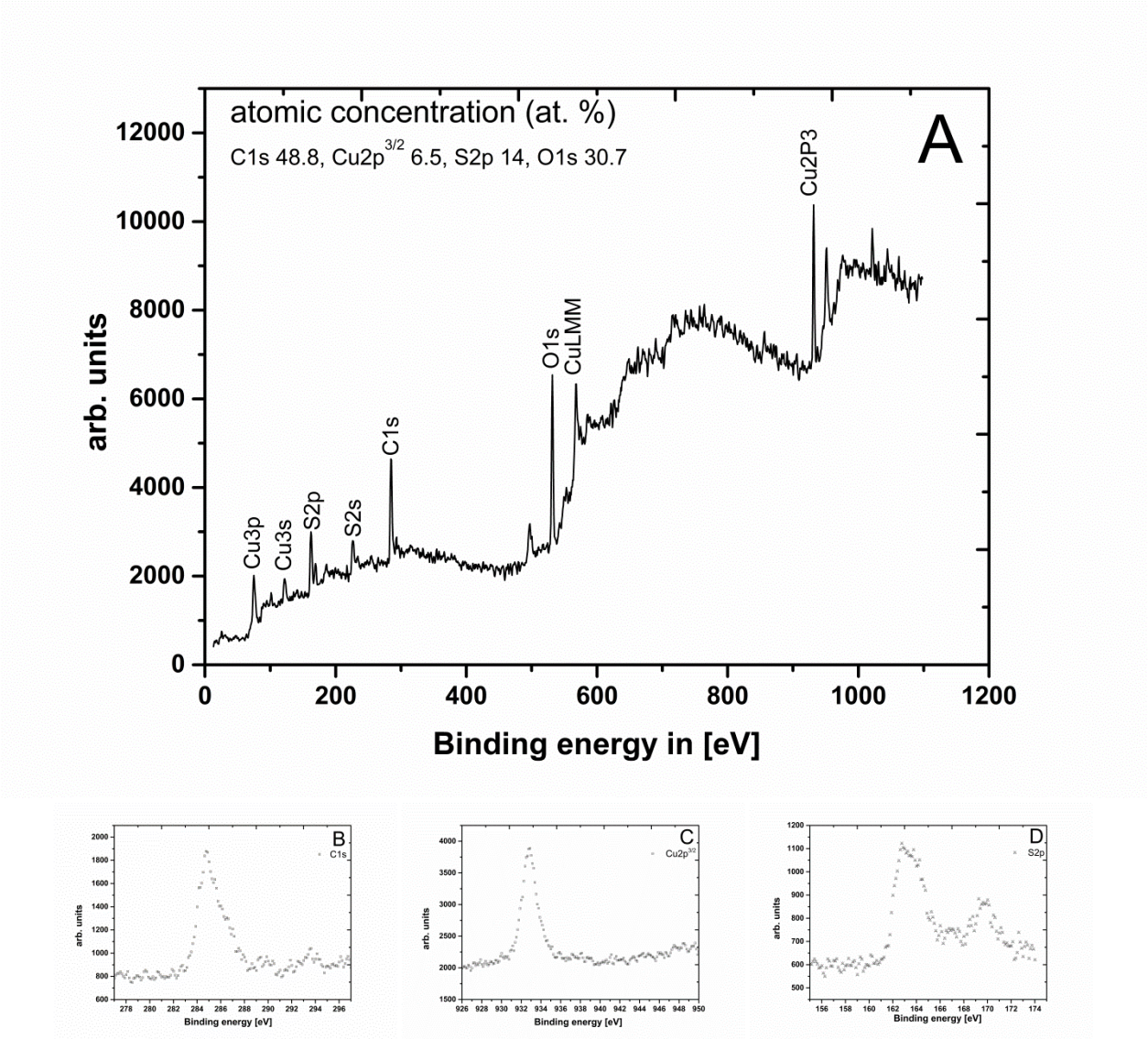


Figure 6: (A) XPS survey spectrum of $H_2S$ exposed sensor B with print density of 2601 drops / $mm^2$, and high resolution spectra of (B) carbon 1s (C) copper $2p^{3/2}$ and (D) sulfur 2p peak.

## 5 Conclusions

The performance of inkjet-printed copper acetate based $H_2S$ gas sensor on a flexible plastic substrate was tested and optimized by varying the ink composition and print density. The long term stability of these sensors after exposure to $H_2S$ was studied extensively. It was observed that the sensing films (formulation B) with print density of 2601 and 1681 drops / $mm^2$ were most

stable and showed no change in resistance during the storage time of 30 days in ambient conditions. Furthermore, surface plasma treatment of the substrate before printing did not show any effect on the sensing response. Hence, these films are ideal (in terms of stability, response time, onset time of detection and sensing kinetics) to be integrated with low-cost wirelessly readable printed RLC-circuitry which can be used e.g. for monitoring the quality of raw poultry. It is concluded that single nozzle printing or multiple nozzle printing (up to four nozzles) of these sensing films make no transformation in sensor performance.

## 6 Acknowledgement

The authors would like to thank the financial support from the Academy of Finland through ICT-programme grant number: 284961 and the ERDF funding through project PAKKAAMO 2020. Helka Juvonen is acknowledged for viscosity measurement of formulation C.

---

[1] B. Doujaiji , j. Al-Tawfiq, Hydrogen sulfide exposure in an adult male, Ann Saudi Med. 30 ( 2010) 76 - 80.

[2] S. Rosolina, T. Carpenter, and Z. Xue, Bismuth-Based, Disposable Sensor for the Detection of Hydrogen Sulfide Gas, Anal. Chem., 88 (2016) 1553 - 1558.

[3] J. Tamaki, T. Maekawa, N. Miura, N. Yamazoe, CuO-$SnO_2$ element for highly sensitive and selective detection of $H_2S$, Sens. Actuators B: Chem. 8 (1992)197 - 203.

[4] Y. Nie, P. Deng, Y. Zhao, P. Wang, L. Xing, Y. Zhang, X. Xue, The conversion of PN-junction influencing the piezoelectric output of a CuO/ZnO nanoarray nanogenerator and its application as a room-temperature self-powered activeH2S sensor, Nanotechnology 25 (2014) 265501.

[5] S. Zhang, P. Zhang, Y. Wang, Y. Ma, J. Zhong, X. Sun, Facile fabrication of a well-ordered porous Cu-doped $SnO_2$ thin film for $H_2S$ sensing, ACS Appl.Mater. Interfaces 6 (2014) 14975-14980.

[6] K. Crowley, E. O'Malley, A. Morrin, M.R. Smyth, A.J. Killard, An aqueous ammonia sensor based on an inkjet-printed PANI nanoparticle-modified electrode, Analyst 133 (2008) 391 - 399.

[7] J. Sarfraz, P. Ihalainen, A. Määttänen, R. Bollström,T. Gulin-Sarfraz, J. Peltonen, M. Lindén, Stable ink dispersions suitable for roll-to-roll printing with sensitivity towards hydrogen sulphide gas, Colloids and Surfaces A: Physicochem. Eng. Aspects 460 (2014) 401 - 407

[8] J. Sarfraz, P. Ihalainen, A. Määttänen, J. Peltonen, M. Lindén, Printed hydrogensulfide gas sensor on paper substrate based on polyaniline composite, ThinSolid Films 534 (2013) 621 - 628.

[9] L.R. Freeman, G.J. Silverman, P. Angelini, C. Merritt, W.B. Esselen, Volatiles pro-duced by microorganisms isolated from refrigerated broiler at spoilage, Appl.Environ. Microbiol. 32 (1976) 222–231.

[10] M. Eilamo, A. Kinnunen, K. Latva-Kala, R. Ahvenainen, Effects of packaging andstorage conditions on volatile compounds in gas-packed poultry meat, FoodAddit. Contam. 15 (1998) 217–228.

[11] S.H. Viehweg, R.E. Schmitt, W. Schmidt Lorenz, Microbial spoilage of refrig-erated fresh broilers, Part VII, Production of off odours from poultry skin bybacterial isolates, Lebensm.-Wiss. Technol. 22 (1989) 356–367.

[12] S. Virji, R. Kaner, B. Weiller, Direct electrical measurement of the conversion of metal acetates to metal sulfides by hydrogen sulfide, Inorganic Chemistry 45 (2006) 10467 - 10471.

[13] D. Skoog, D.M. West, Analytical Chemistry an Introduction, Holt, Rinehart and Winston, New York, 1965.

[14] K. Osakada, A. Taniguchi, E. Kubota, S. Dev, K. Tanaka, K. Kubota, T. Yamamoto, New organosols of copper(II) sulfide, cadmium sulfide, zinc sulfide, mercury(II) sulfide, nickel(II) sulfide and mixed metal sulfides in N,N-dimethylformamide and dimethyl sulfoxide. Preparation, characterization, and physical properties, Chemistry of Materials 4 (1992) 562 - 570.

[15] J. Sarfraz, A. Maattanen, B. Törngren, M. Pesonen, J. Peltonen and P. Ihalainen, Sub-ppm electrical detection of hydrogen sulfide gas at room temperature based on printed copper acetate–gold nanoparticle composite films, RSC Adv., 5 (2015) 13525 - 13529.

[16] J. Sarfraz, P. Ihalainen, A. Määttänen, T. Gulin, J. Koskela, C.-E. Wilén, A. Kilpelä,J. Peltonen, A printed $H_2S$ sensor with electro–optical response, Sens. Actuators B 191 (2014) 821 - 827.

[17] J. Sarfraz, A. Määttänen, P. Ihalainen, M. Keppeler, M. Lindén, J. Peltonen, Printed copper acetate based $H_2S$ sensor on paper substrate, Sens. Actuators B 173 (2012) 868 - 873.

[18] J. Koskela, J. Sarfraz, P. Ihalainen, A. Määttänen, P. Pulkkinen, H. Tenhu, T. Nieminend, A. Kilpelä, J. Peltonen, Monitoring the quality of raw poultry by detecting hydrogen sulfide with printed sensors, Sens. Actuators B 218 (2015) 89 - 96.

[19] J. Fromm, Numerical-calculation of the fluid-dynamics of drop-on-demand jets. IBM J. Res. Dev. 28 (1984) 322 - 333.

[20] N. Reis, B. Derby, Ink jet deposition of ceramic suspensions: Modelling and experiments of droplet formation, Materials Development for Direct Write Technologies, Boston, MA, 2000, Materials Res. Soc. Symp. Proc. 624 (2000) 65 - 70.

[21] D. Jang, D. Kim, J. Moon, Influence of fluid physical properties on ink-jet printability, Langmuir 25 (2009) 2629 - 2635.

[22] Jawad Sarfraz, Mykola Borzenkov, Erik Niemelä, Christian Weinberger, Björn Törngren, Emil Rosqvist, Maddalena Collini, Piersandro Pallavicini, John Eriksson, Jouko Peltonen, Petri Ihalainen, Giuseppe Chirico, Photo-thermal and cytotoxic properties of inkjet-printed copper sulfide films on biocompatible latex coated substrates, Applied Surface Science 435 (2018) 1087 – 1095.

[23] K. Benkstein, S. Semancik, Mesoporous nanoparticle $TiO_2$ thin films for conductometric gas sensing on micro hotplate platforms, Sens. Actuators, B 113 (2006) 445 - 453.

[24] Qian Xu , Jan-Henrik Smått, Jouko Peltonen and Petri Ihalainen, Fabrication of nanoperforated ultrathin TiO2 films by inkjet printing, J. Matter. Res., 30 (2015) 2151 – 2160.

[25] P.C. Duineveld : The stability of ink-jet printed lines of liquid with zero receding contact angle on a homogeneous substrate. J. Fluid Mech. 477 (2003) 175 – 200.

[26] D. Soltman and V. Subramanian : Inkjet-printed line morphologies and temperature control of the coffee ring effect. Langmuir 24 (2008) 2224 – 2231.

[27] B. Strohmeier, D. Leyden, R. Scottfield, D. Hercules, Surface spectroscopic characterization of Cu $Al_2O_3$ catalysts, Journal of Catalysis 94 (1985) 514 - 530.

[28] J. Moulder, W. Stickle, P. Sobol, K. Bomben, in: J.J. Chastain (Ed.), Handbook of X-ray Photoelectron Spectroscopy, 2nd ed., Perkin Elmer Corporation, Physical Electronics, 1992, and references therein.

[29] V. Bhide, S. Salkalachen, A. Restogi, C. Rao, M. Hegde, Depth profile composition studies of thin film CdS:$Cu_2S$ solar cells using XPS and AES, Journal of Physics D: Applied Physics 14 (1981) 1647 - 1656.

[30] X. Yu, F. Liu, Z. Wang, Y. Chen, Auger parameters for sulfur-containing compounds using a mixed aluminum–silver excitation source, Journal of Electron Spectroscopy and Related Phenomena 50 (1990) 159 - 166.